

Supramolecular photocatalyst of Palladium (II) Encapsulated within Dendrimer on TiO₂ nanoparticles for Photo-induced Suzuki-Miyaura and Sonogashira Cross-Coupling reactions

Ameneh Eskandari  | Maasoumeh Jafarpour  | Abdolreza Rezaeifard  | Mehri Salimi 

Catalysis Research Laboratory,
Department of Chemistry, Faculty of
Science, University of Birjand, Birjand
97179-414, Iran

Correspondence

Maasoumeh Jafarpour and Abdolreza
Rezaeifard, Catalysis Research Laboratory,
Department of Chemistry, Faculty of
Science, University of Birjand, Birjand,
97179-414 Iran.

Email: mjafarpour@birjand.ac.ir;
jafarpouryas@gmail.com;
rezaeifard@gmail.com;
rezaeifard@birjand.ac.ir

In this study, synthesis, characterization and catalytic performance of a novel supramolecular photocatalytic system including palladium (II) encapsulated within amine-terminated poly (triazine-triamine) dendrimer modified TiO₂ nanoparticles (Pd (II) [PTATAD] @ TiO₂) is presented. The obtained nanodendritic catalyst was characterized by FT-IR, ICP-AES, XPS, EDS, TEM, TGA and UV-DRS. The as-prepared nanodendritic catalyst was shown to be highly active, selective, and recyclable for the Suzuki–Miyaura and Sonogashira cross-coupling of a wide range of aryl halides including electron-rich and electron-poor and even aryl chlorides, affording the corresponding biaryl compounds in good to excellent yields under visible light irradiation. This study shows that visible light irradiation can drive the cross-coupling reactions on the Pd (II) [PTATAD] @ TiO₂ under mild reaction conditions (27–30 °C) and no additional additives such as cocatalysts or phosphine ligands. So, we propose that the improved photoactivity predominantly benefits from the synergistic effects of Pd (II) amine-terminated poly (triazine-triamine) dendrimer on TiO₂ nanoparticles that cause efficient separation and photogenerated electron–hole pairs and photoredox capability of nanocatalyst which all of these advantages due to the tuning of band gap of catalyst in the visible light region.

KEYWORDS

cross-coupling reactions, nanodendritic catalyst, Pd (II) dendrimers, photocatalyst, poly (triazine-triamine) dendrimer

1 | INTRODUCTION

C-C coupling reactions are great importance in various organic transformation, polymer synthesis, and pharmaceuticals intermediates.^[1–3] C-C bonds can be formed via palladium-catalyzed coupling reactions, such as the Suzuki-Miyaura, Sonogashira and Heck

reactions.^[4–10] The redox processes in the C-C coupling reactions occur through electron transfer between transition metal catalysts and organic substances, which typically requires elevated temperatures or sacrificial reagents.^[11,12] However, electron transfer-mediated C-C coupling can also be improved by visible light at room temperature in the presence of photocatalysts.^[3,13–18]

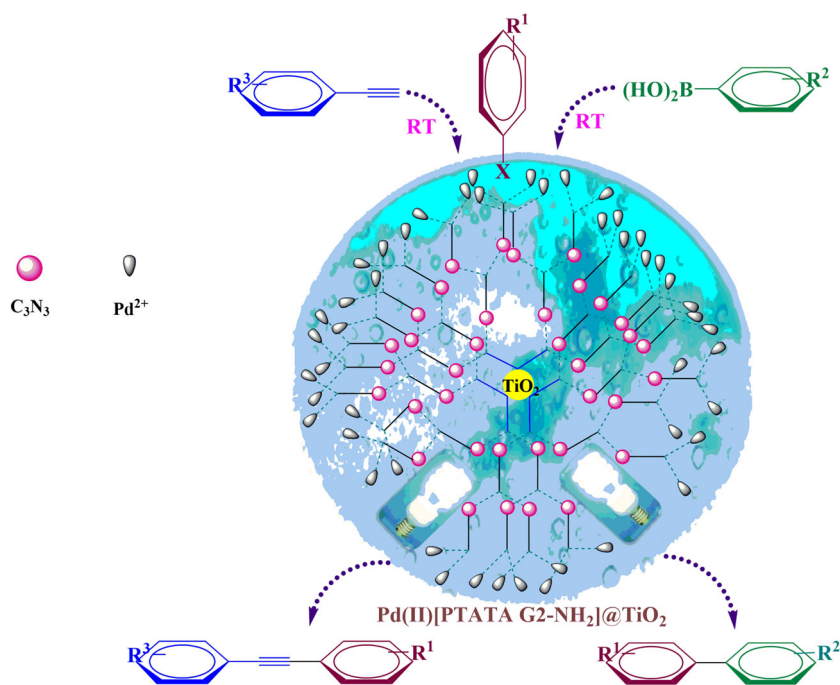
Hence, efficient harvesting of solar energy is promising and has been a worldwide high priority target.^[19] Diverse artificial light-harvesting techniques have been applied to drive chemical reactions.^[20,21] Semiconductors, one types of photocatalysts is widely employed in photoredox reactions.^[22–26] The energy band gap has an energy range similar to that of visible light when to absorb to an incident photon, generate an electron–hole pair to facilitate its separation and act as electron donors and acceptors, whereas catalysis of the reaction is an additional function which is usually performed by different materials. In particular, semiconductors are utilized as photocatalysts for organic transformations because of effective absorption of visible light, good durability, capacity for multivalent binding to substrates. Among semiconductors, titanium dioxide (titania) was selected due to both potential and demonstrated applications in solar energy conversion,^[27–29] photocatalysis,^[30–32] and photochromic devices.^[33,34] Also, hybrid photocatalysts integrate the synergistic effects between the individual components for increased light harvesting, prolonged lifetime, enhanced photocatalytic performance as well as higher chemical and environmental stability. TiO₂-based hybrid photocatalysts can be classified into two main categories according to the type of species added: polymers include dendrimers and carbon nanomaterials.^[35] The design of dendritic catalysts has mostly concerned because of highly branched three-dimensional structures and strong encapsulation of transition metal onto the termini of dendritic tethers or at the dendrimer core.^[36–41]

The N-H moieties as the ligand in organometallic dendrimers catalysts can serve as coordination groups

because these are readily available, chemically stable and easily introduced to the ligands. Therefore, the N-H moiety is the ideal functional group for the formation of multifunctional catalysts. In addition, the synthesis of dendrimers based on melamine and triazines interconnected with diamines, aim to reduce many of the synthetic challenges to compositional diversity to the trivial.^[42]

Also, the use of metal-containing dendritic polymers immobilized on solid supports has practical importance in the field of catalysis because of their easy recovery of the nanocatalysts and multiple recycling and continuous processing. Owing to these advantages, heterogeneous dendritic polymer-based catalysts have been investigated in many important organic transformations.^[43–46]

With this goal in mind, in continuous our studies to development of novel strategies for the organic transformation,^[47–52] we modified band gap of TiO₂ nanoparticles by Pd (II) amine-terminated poly (triazine-triamine) dendritic which induced outstanding photocatalytic activity in Suzuki-Miyaura and Sonogashira cross-coupling reactions at room temperature under visible light (Scheme 1). These results proposed that the improved photoactivity predominantly benefits from the synergistic effects of Pd (II) amine-terminated poly (triazine-triamine) dendritic on TiO₂ nanoparticles that cause efficient separation and photogenerated electron–hole pairs and photoredox capability of nanocatalyst which all of these advantages due to the tuning of band gap of catalyst in the visible light region. It should be noted that there are many reports of cross-coupling reactions catalyzed via homogeneous or heterogeneous processes, but most of



SCHEME 1 Suzuki-Miyaura and Sonogashira cross-coupling reactions by Pd (II) [PTATAD] @ TiO₂

them need to be conducted at elevated temperatures (≥ 100 °C), even under reflux conditions.^[53–62] This study shows that visible light irradiation can drive the same reactions on the Pd (II) [PTATAD] @ TiO₂ under much milder reaction conditions (27–30 °C), achieving good to excellent yields, and no additional additives such as co-catalysts or phosphine ligands are required.

2 | EXPERIMENTAL

Note: See General remarks and step by step preparation of Pd (II) [PTATAD] @ TiO₂ catalyst in supporting information.

2.1 | General procedure for Suzuki-Miyaura cross-coupling catalyzed by Pd (II) [PTATAD] @ TiO₂ catalyst

A mixture of aryl halide (0.125 mmol), arylboronic acid (0.126 mmol), K₂CO₃ (0.187 mmol) and Pd (II) [PTATAD] @ TiO₂ (1.46 mol%) in 0.5 ml of H₂O/EtOH (1:1) was stirred at room temperature (27–30 °C) for the period of time indicated in Table 1. The progress of the reaction was monitored by TLC. After completion of the reaction, Pd (II) [PTATAD] @ TiO₂ was separated by centrifuging followed by decantation EtOAc (3 × 0.5 ml). Then the organic phase dried over anhydrous MgSO₄. The solvent was evaporated by vacuum and the residue was recrystallized from ethyl acetate to afford the pure product (Table 1).

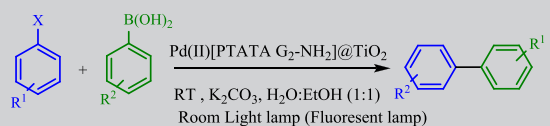
2.2 | General procedure for Sonogashira cross-coupling catalyzed by Pd (II) [PTATAD] @ TiO₂ catalyst

A mixture of aryl halide (0.125 mmol), phenylacetylene (0.137 mmol), Et₃N (0.125 mmol) and Pd (II) [PTATAD] @ TiO₂ (0.35 mol%) in 0.1 ml of H₂O was stirred at room temperature for the period of time indicated in Table 2. The reaction progress was monitored by TLC (with adding EtOAc). After completion of the reaction, Pd (II) [PTATAD] @ TiO₂ was separated by centrifuging followed by decantation EtOAc (3 × 0.5 ml). The desired products were obtained by evaporation of solvent of organic phase to afford the pure product (Table 2).

2.3 | Reusability of catalyst

A mixture of iodobenzene (0.125 mmol), phenylboronic acid (0.126 mmol) [for sonogashira Cross-coupling: phenylacetylene (0.137 mmol)], K₂CO₃ (0.187 mmol)

TABLE 1 The Suzuki-Miyaura cross-coupling of aryl halides with arylboronic acids catalyzed by Pd (II) [PTATA G₂-NH₂] @ TiO₂^a



Entry	X	R ¹	R ²	Time (min)	Isolated Yield(%) ^b
1	I	H	H	30	96
2	I	<i>p</i> -NO ₂	H	60	55
3	I	<i>p</i> -OMe	H	60	72
4	I	<i>p</i> -Me	H	60	95
5	I	<i>o</i> -Me	H	90	83
6	Br	H	H	60	95
7	Br	<i>p</i> -NO ₂	H	120	55
8	Br	<i>p</i> -OMe	H	120	65
9	Cl	H	H	60	64
10	Cl	<i>p</i> -NO ₂	H	150	52
11 ^c	I	<i>p</i> -Br	H	180	46:46 ^d
12 ^c	I	<i>p</i> -I	H	120	53 ^e
13	I	H	<i>p</i> -CHO	120	72
14	I	H	<i>p</i> -Cl	60	94
15	I	H	<i>p</i> -OMe	60	92
16	I	H	<i>p</i> -Et	30	92
17	I	H	<i>m</i> -NO ₂	90	81
18	I	H	2- thienylboronic acid	90	15
19 ^f		C ₃ N ₃ Cl ₃	H	60	92

^aReaction conditions: 1.25: 1.26: 1.87: 14.6 molar ratio for arylhalides: phenylboronic acids: K₂CO₃: catalyst, H₂O: EtOH (1:1) (0.5 ml) at room temperature.

^bIsolated Yield.

^cReaction conditions: 1-bromo-4-iodobenzene or 1,4-diiodobenzene (0.125 mmol), arylboronic acid (0.25 mmol), K₂CO₃ (0.37 mmol), Pd (II) [PTATA G₂-NH₂]@TiO₂ (2.92 mol%), H₂O: EtOH (1: 1) (1 mL) at room temperature.

^dMixture of *para*-Terphenyl and 4-bromobiphenyl.

^e*para*-Terphenyl (100% selectivity).

^f2,4,6-trichlorotriazine (0.125 mmol), arylboronic acid (0.37 mmol), K₂CO₃ (0.54 mmol), Pd (II) [PTATA G₂-NH₂]@TiO₂ (4.38 mol%), H₂O: EtOH (1: 1) (1 mL) at room temperature.

[Et₃N (0.125 mmol)] and Pd (II) [PTATAD] @ TiO₂ (1.46 mol%) [(0.35 mol%)] in 0.5 mL of H₂O/EtOH (1:1) [in 0.1 mL of H₂O] was stirred at room temperature for 30 min [180 min]. After completion of the reaction, Pd (II) [PTATAD] @ TiO₂ was separated by centrifuging followed by decantation EtOAc (5 × 0.5 ml). The isolated solid phase Pd (II) [PTATAD] @ TiO₂ was dried under reduced pressure and reused for next runs.

TABLE 2 The Sonogashira cross-coupling of aryl halides with phenylacetylenes catalyzed by Pd (II) [PTATA G₂-NH₂] @ TiO₂^a

Entry	X	R ¹	R ²	Time(h)	Isolated Yield(%) ^b
1	I	H	H	3	98
2	I	<i>p</i> -Me	H	2	85
3	I	<i>o</i> -Me	H	2.5	68
4	I	<i>p</i> -NO ₂	H	3	20
5	I	<i>p</i> -OMe	H	3	35
6	Br	H	H	6	72
7	Br	<i>p</i> -NO ₂	H	6	15
8	Br	<i>p</i> -OMe	H	6	25
9	Cl	H	H	6	40
10 ^c	I	<i>p</i> -Br	H	6	80 ^d
11 ^c	I	<i>p</i> -I	H	6	20:20 ^e
12	I	H	<i>p</i> -Me	3	90
13 ^f	C ₃ N ₃ Cl ₃	H	H	5	90
14	I	H	2-Methyl -3-butyn -2-ol	24	85
15	I	H	1-Hexyne	24	No product

^aReaction conditions: 1.25: 1.37: 1.25: 3.5 molar ratio for aryl halides: phenylacetylenes: Et₃N: catalyst, H₂O (0.1 ml) at room temperature.

^bIsolated Yield.

^cReaction conditions: 1-bromo-4-iodobenzene, 1,4-diiodobenzene (0.125 mmol), phenylacetylene (0.274 mmol), Et₃N (0.25 mmol), Pd (II) [PTATA G₂-NH₂]@TiO₂ (0.7 mol%), H₂O (0.2 mL) at room temperature.

^d1-bromo-4-(phenylethynyl) benzene (100% selectivity).

^eMixture of 1,4-bis (phenylethynyl)benzene and 1-iodo-4-(phenylethynyl) benzene.

^f2,4,6-trichlorotriazine (0.125 mmol), phenylacetylene (0.411 mmol), Et₃N (0.375 mmol), Pd (II) [PTATA G₂-NH₂] @TiO₂ (1.05 mol%), H₂O (0.3 mL) at room temperature.

3 | RESULT AND DISCUSSION

3.1 | Synthesis and characterization of Pd (II) [PTATAD] @ TiO₂ catalyst

As shown in Scheme 2, organosilicon diester A was prepared by condensation of organosilicon aldehyde 1 with diethylmalonate under ultrasonic agitation which in continued was used as an appropriate linker for a new heterogeneous supported catalyst and a bifunctional molecule for growing of dendritic branches. In the ¹H NMR spectrum (Figure S1), hydrogens (H_a) of the two methyl groups of ethyl part appeared at 1.161 ppm, while hydrogens (H_b) of the two methylene groups the ethyl part

appeared at 4.01 ppm. The two broad peaks at 1.77 and 0.77 ppm are corresponding to methylene groups (H_c, H_d). A peak at 2.8 ppm and 3.5 ppm in the spectrum assigned to C-H_f and C-H_e, respectively. The hydrogen of -OMe groups is masked due to the presence of solvent peak.

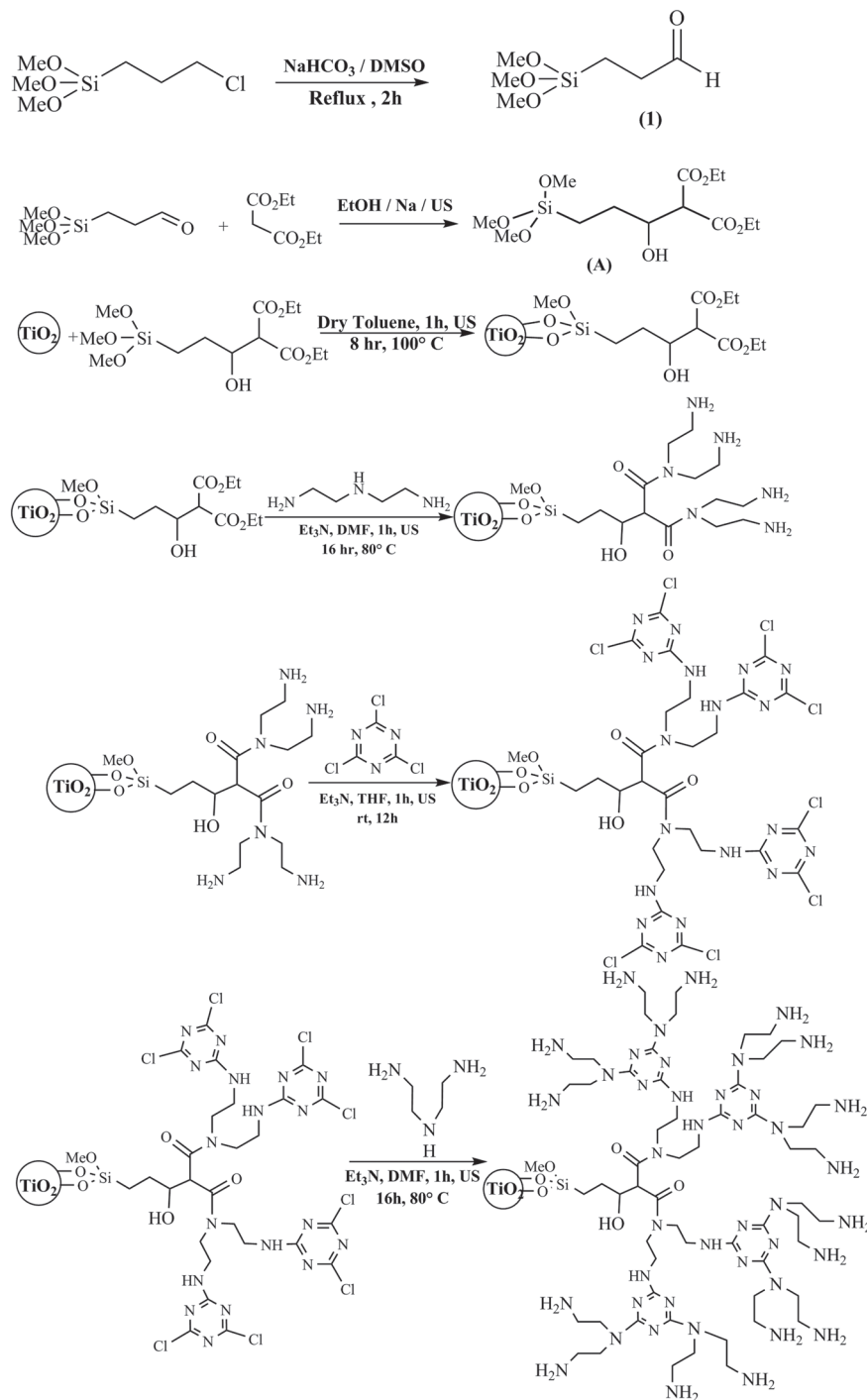
In Figure 1a, the strong peaks centered at 1726 and 1242 cm⁻¹ can be assigned to the characteristic for (C=O) and (C - O) ester groups vibrations. Characteristic bands observed for organosilicon compound at 1155 cm⁻¹ (Si - O bend) and 1029 cm⁻¹ (Si - O stretch) and CH₂ groups asymmetrical stretching was obtained at 2980 cm⁻¹.

Then, as-prepared organosilicon diester was immobilized on TiO₂ nanoparticles of approximately 18–20 nm diameters.^[63] New poly (triazine-triamine) dendrimer was synthesized using two building blocks, diethylenetriamine (DETA) and cyanuric chloride (CC), alternatively. The reaction of diethylenetriamine with organosilicon diester supported on TiO₂ and then with cyanuric chloride and diethylenetriamine respectively, gave the first generation dendrimer, G1-NH₂. The FT-IR spectrum of the synthesized dendrimer G1 (Figure 1b) showed absorption peaks at 3550–3230 cm⁻¹ which can be rationalized to N-H asymmetric stretching of primary amine and O-H stretches (H₂O and Ti - OH). The peaks at 1637 and 1614 cm⁻¹ belong to amide groups, C=N in cyanuric ring. The presence of major bands at 507–617 cm⁻¹ is attributed to the stretching vibrations of Ti-O groups.

The second generation dendron was obtained by reaction of G1-NH₂ with cyanuric chloride and diethylenetriamine, respectively. Finally, Pd (II) [PTATA G₂-NH₂] @ TiO₂ was prepared by incorporating of Pd (OAc)₂ into [PTATA G₂-NH₂] coated TiO₂ nanoparticles that has been dispersed in DMF under ultrasonic agitation. Figure 1c demonstrates significant spectral changes in the FT-IR spectra of Pd (II) [PTATA G₂-NH₂] @ TiO₂ compared with those of organosilicon diester and G1-NH₂ (Figure 1a,b). The stretching frequency at 528 cm⁻¹ in the spectrum of Pd (II) [PTATA G₂-NH₂] @TiO₂ (Figure 1c) indicates Pd-N bond^[60,64] confirming the complexation of Pd with [PTATA G₂-NH₂] coated TiO₂ nanoparticles which the stretching vibrations of Ti-O groups are shifted.

The as-prepared Pd (II) [PTATA G₂-NH₂] @TiO₂ was analyzed by ICP-AES and the Pd loading was found to be 1.83 mmol.g⁻¹ (19.51 wt%).

X-ray photoelectron spectroscopy (XPS) was applied to assess the chemical composition of macromolecules and their oxidation states. The XPS spectrum of Pd (II) [PTATA G₂-NH₂] @TiO₂ in Figure S2 a, the characteristic binding energies of C 1 s, O 1 s, N 1 s, Ti 2p, Si 2p and Pd 3d are identified according to C 1 s photoelectron peak as reference



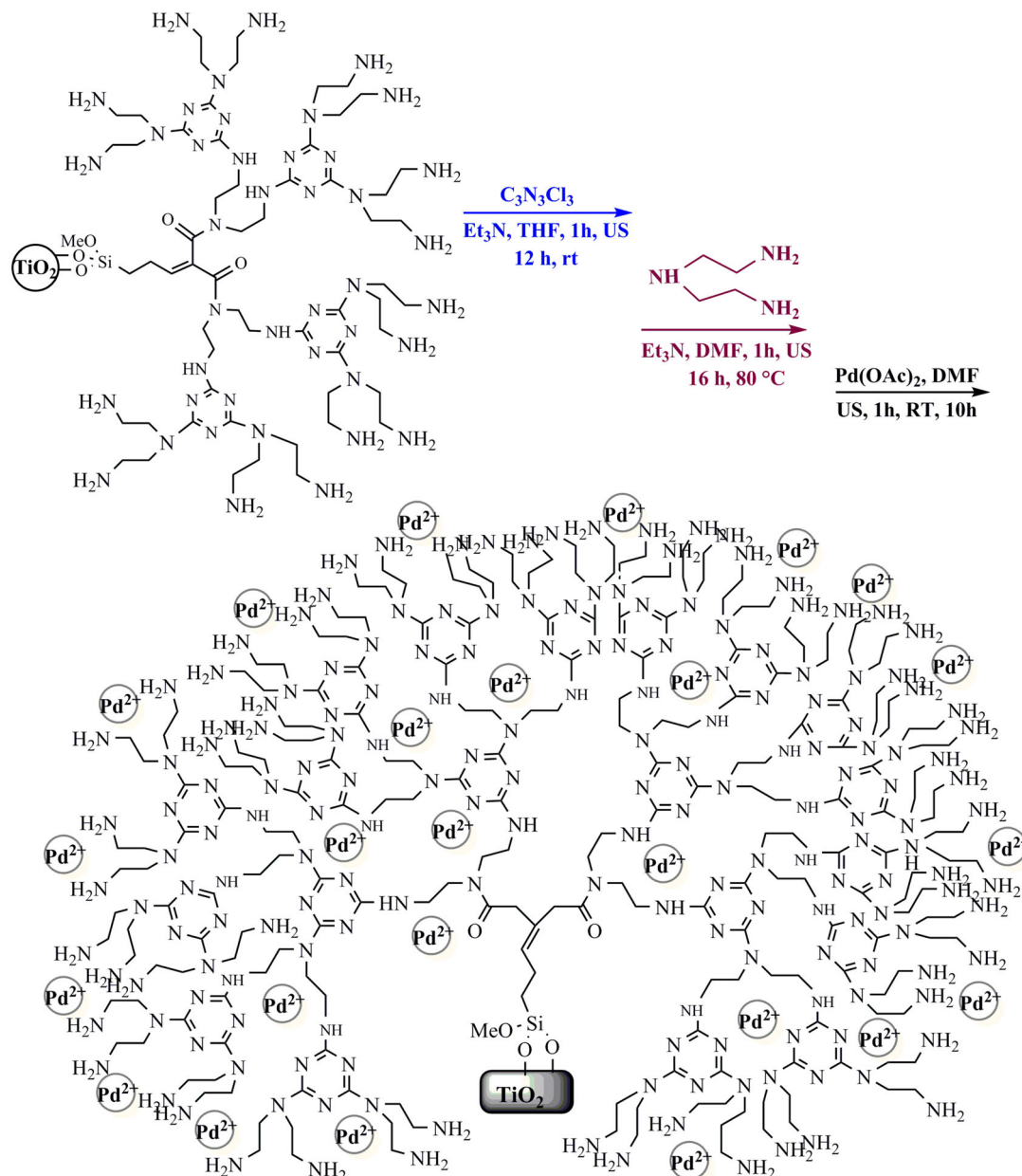
SCHEME 2 Preparation route for Pd (II) [PTATA G2-NH₂] @ TiO₂

(285 eV). The XPS analysis shows Pd (II) in the catalyst with two intense peaks at 337.98 eV and 343.18 eV, corresponding to Pd_{3/2} and Pd_{5/2} in Figure S2 b. As can be seen, the BE of 337.98 eV for the Pd (II) species in Pd (II) [PTATA G2-NH₂] @ TiO₂ shifted negatively by 0.42 eV in comparison with that of 338.4 eV for free Pd (OAc)₂. Also, in Figure S2 d, a positive shift of the binding energy for N 1 s spectrum of the primary amines in Pd (II) [PTATA G2-NH₂] @ TiO₂ in comparison with N 1 s spectrum of

no coordinated the primary amine (398.1 to 399.68) was observed. These above observations indicate the strong coordination of Pd (OAc)₂ with [PTATA G2-NH₂] @ TiO₂.

Also, the elemental composition of Pd (II) [PTATA G2-NH₂] @ TiO₂ nanodendritic catalyst was clarified by EDS (see Figure S3 in supporting information) that was in agreement with the XPS results of nanodendritic catalyst.

Transmission electron microscopy (TEM) was also investigated for characterization of Pd (II) [PTATA



SCHEME 2 Continued.

G2-NH_2] @ TiO_2 . The TEM images of Pd (II) [PTATA G2-NH_2] @ TiO_2 clearly showed spherical morphology with size ranging between 70–80 nm in Figure S4.

The thermal stability of G2-NH_2 and nanodendritic catalyst are studied by thermogravimetric analysis. The G2-NH_2 and Pd (II) [PTATA G2-NH_2] @ TiO_2 nanodendritic catalyst were completely decomposed above 700 °C (see Figure S5 in supporting information).

The diffuse reflectance UV–Vis spectra of the G2-NH_2 and Pd (II) [PTATA G2-NH_2] @ TiO_2 nanodendritic catalyst are shown in Figure 2. Both of samples (G2-NH_2 and Pd (II) [PTATA G2-NH_2] @ TiO_2) were red shifted and extended absorption in the visible-light region, so

as-prepared samples showed visible light absorption, especially in the wavelength range from 400 to 600 nm. For the Pd (II) [PTATA G2-NH_2] @ TiO_2 nanodendritic catalyst, the absorption band was found at around 421 nm and 516 nm. The absorption coefficient, could be calculated according to the Kubelka–Munk method based on the diffuse reflectance spectra, the estimated band gap energies for the TiO_2 , G2-NH_2 and Pd (II) [PTATA G2-NH_2] @ TiO_2 nanodendritic are 3.15, 2.95 and 2.92 eV, respectively. It can be seen that the band gap energies found for the Pd (II) [PTATA G2-NH_2] @ TiO_2 nanodendritic is lower than TiO_2 and G2-NH_2 . Therefore, band gap of TiO_2 has been modified by

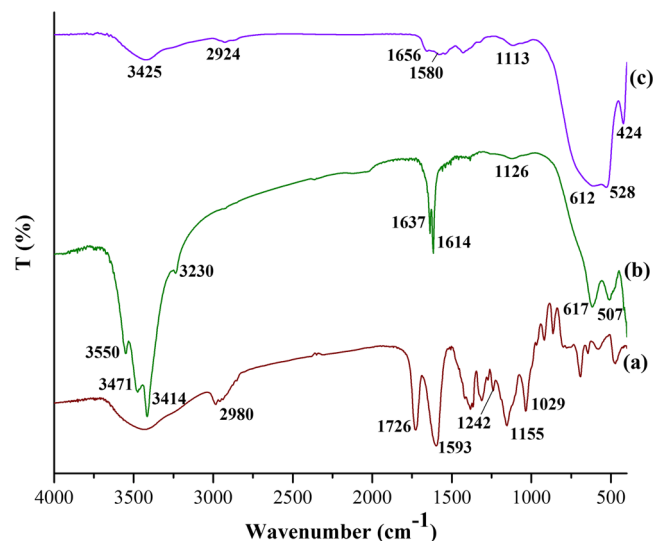


FIGURE 1 FT-IR spectra of (a) organosilicon diester, (b) G1-NH₂ (c) Pd (II) [PTATA G2-NH₂] @ TiO₂

Palladium (II) encapsulated within amine-terminated poly (triazine-triamine) dendrimer which induces visible light activity in TiO₂.

3.2 | Photo-induced Suzuki-Miyaura and Sonogashira cross-coupling reactions under visible light irradiation at room temperature

Whereas, catalysts containing palladium are known to be an active species able to promote cross coupling reactions effectively and based on the tuning of band gap of as-prepared catalyst in the visible light region (Figure 2), we decided to describe catalytic potential of title nanodendritic catalyst for photo-induced Suzuki-Miyaura and Sonogashira cross-coupling reactions.

At the outset of our study, iodobenzene and phenylboronic acid were chosen as model substrates to optimize the reaction conditions such as various bases, solvents, temperature, catalyst loading under room light irradiation (Fluorescent Lamp) (Figure S6) and different palladium sources (Figure S7).

Among the various solvents studied, mixed solvent of H₂O:EtOH (0.25: 0.25) and H₂O:DMF (0.25: 0.25) in the presence of 1.46 mol% catalyst and 0.180 mmol of K₂CO₃ at room temperature (27–30 °C) gave excellent conversion (Figure S6 i).

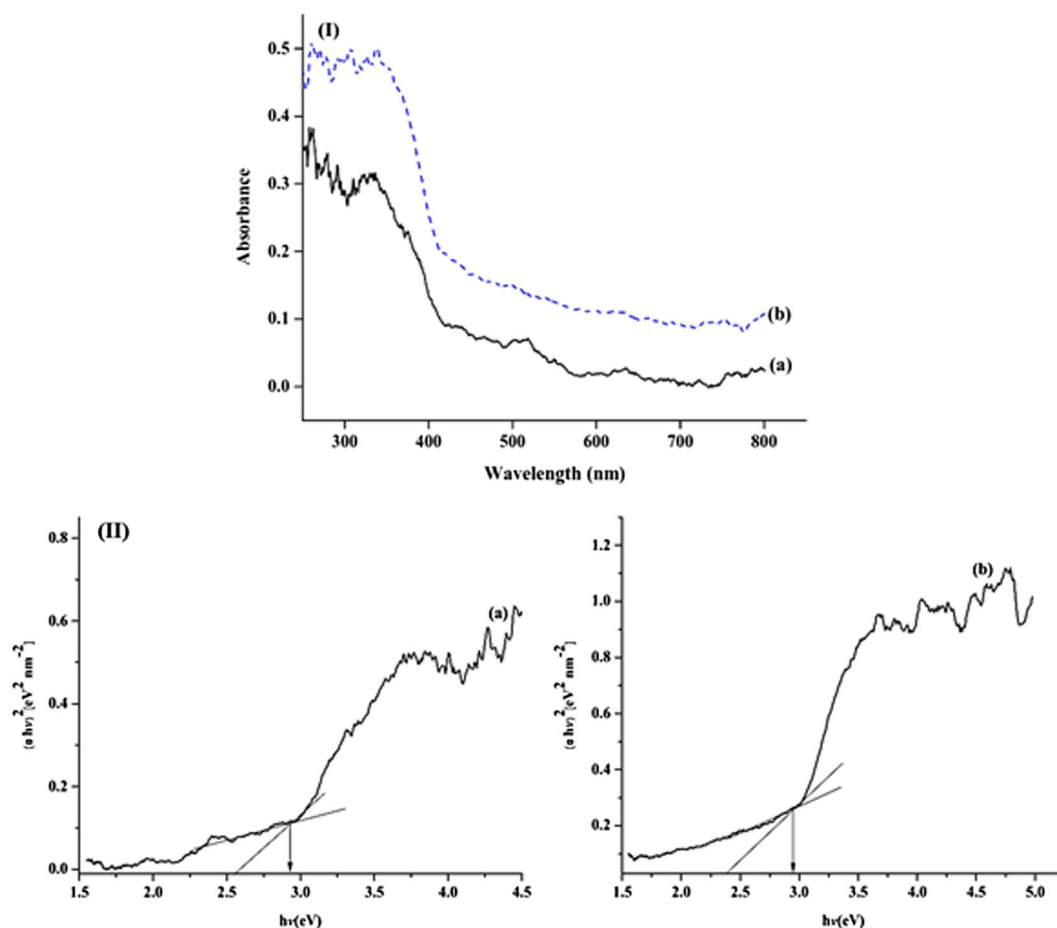


FIGURE 2 Diffuse reflectance UV-vis spectra of (a) G2-NH₂ (b) Pd (II) [PTATA G2-NH₂] @TiO₂ nanodendritic catalyst

The effect of various bases was studied for the reaction between iodobenzene and phenylboronic acid. The study of different bases shows that K_2CO_3 was the best base among the bases (Figure S6 v). The reaction was further optimized with respect to different palladium concentrations (Figure S6 iv), solvent (Figure S6 ii) and base amount (Figure S6 vi).

On the basis of the experiments above, the best reaction conditions for cross coupling of iodobenzene (0.125 mmol) and phenylboronic acid (0.126 mmol) was obtained in the presence of 1.46 mol% Pd (II) [PTATA G2-NH₂] @TiO₂ nanodendritic catalyst and 0.187 mmol K_2CO_3 at room temperature (27–30 °C) in 0.5 mL H₂O: EtOH (0.25: 0.25) within 30 min under visible light irradiation.

In continued, we found that the performance of the nanodendritic photocatalyst depends on the core type which acts as support, dendritic branches, and light wavelength.

Pd (II) [PTATA G2-NH₂] nanodendritic supported on MoO₃ and SMNP (starch coated γ -Fe₂O₃) as control experiments led to less yields of the product. Using Pd (II) [PTATA G1-NH₂] @TiO₂ nanodendritic as photocatalyst led to a conversion of 80%, indicating that growing of dendritic branches in nanodendritic catalysts effect on photocatalytic activity. So, considering the results presented in Figure S7, the catalytic performance of by Pd (II) [PTATA G2-NH₂] @ TiO₂ nanodendritic catalyst can be explained with respect to catalytic C-C coupling activity of Pd (II) centers^[52,65] combined with photocatalytic activity of TiO₂ core which acts as support and the number of dendritic branches.

Figure 3 shows the relative contributions of light and thermal processes to the conversion efficiencies in Suzuki-Miyaura cross-coupling iodobenzene (0.125 mmol) with phenylboronic acid (0.126 mmol). Herein, we calculated the contributions of the light irradiation to the conversion efficiency by subtracting the conversion of the reaction in the dark from the overall conversion observed when the system was irradiated at identical reaction conditions. It should be noted that the conversion of the reaction in the dark is regarded as the contribution of thermal effect. When the light sources are Actinic BL lamp ($\lambda = 366\text{--}400$ nm, 15 W), UV light ($\lambda = 200\text{--}290$ nm, 15 W), room light lamps (Fluorescent lamp, $\lambda = 400\text{--}650$ nm, 40 W), LED ($\lambda = 505$ nm, 12 W), and sun light (18 W), the light contributions for Suzuki-Miyaura cross-coupling reaction were 71, 77, 80, 80, 80%, respectively. We can see that room light lamps, sun light and LED have the greater contribution of irradiation to the overall conversion rate. The results clearly show a light dependence of Pd (II) [PTATA G2-NH₂] @TiO₂ nanodendritic catalyst for the cross-coupling reactions.

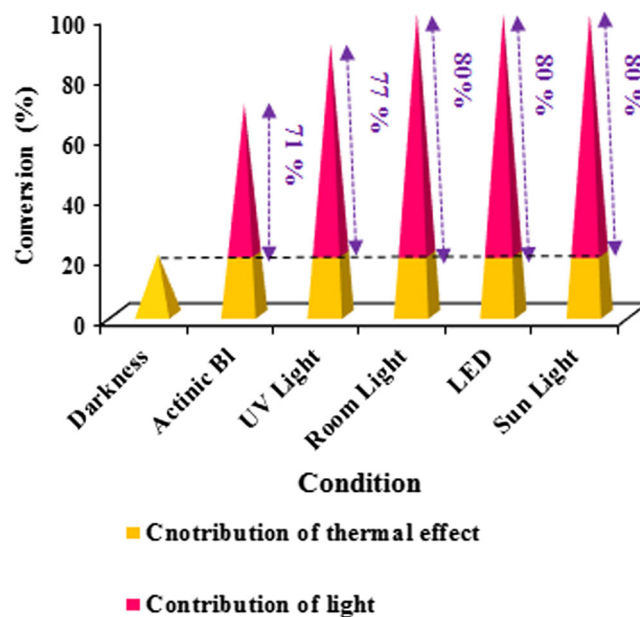


FIGURE 3 Dependence of the catalytic activity of Pd (II) [PTATA G2-NH₂] @ TiO₂ for Suzuki-Miyaura cross-coupling on the irradiation wavelength. The numbers percentages show the contribution of the light irradiation effect. Reaction condition: Iodobenzene (0.125 mmol), Phenylboronic acid (0.126 mmol), Pd (II) [PTATA G2-NH₂] @ TiO₂ (1.46 mol %) in H₂O: EtOH (0.5 ml) at room temperature after 30 min

In Figure 4 was illustrated the dependence of the catalytic activity on the irradiation wavelength. Without any filters, the irradiation of the light with wavelengths ranging from 400 to 800 nm gives a biphenyl yield of 95%. The yield decreases to 79%, 65% and 55% when the wavelength range of the irradiation is 450–800, 520–800, and 600–800 nm, respectively. Since the yield of 4,4-biphenyl in the dark is 20%, the contribution of 400–450 nm light accounts for about 21% $((75-59)/75 \times 100\%)$ in the total light-induced yield. Similarly, the light in the wavelength range of 450–520, 520–600 and 600–800 nm, respectively accounts for 18%, 13% and 20% of the light-induced yield (Figure 4a). These values agree well to the UV–visible absorption spectrum of the Pd (II) [PTATA G2-NH₂] @ TiO₂ catalyst (Figure 4b). Because the Pd (II) [PTATA G2-NH₂] @ TiO₂ nanodendritic catalyst has a strong absorption at about 420 nm, the light in the wavelength range of 400–450 nm contributions the highest light-induced conversion.

The action spectra of Suzuki-Miyaura cross-coupling reaction has been shown in Figure 5. The plot of AQY versus the respective wavelengths is the action spectrum which shows one-to-one mapping between the wavelength-dependent photocatalytic rate and the light extinction spectrum.^[66,67] In this regard, the reaction rates of the synthesis of biphenyl using Pd (II) [PTATA

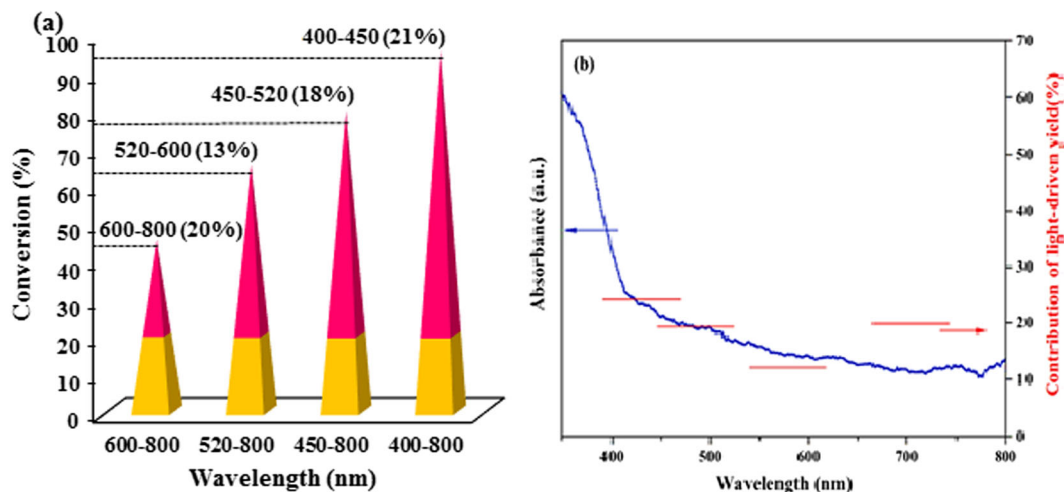


FIGURE 4 The dependence of the catalytic activity of Pd (II) [PTATA G2-NH₂] @ TiO₂ nanodendritic catalyst for the Suzuki-Miyaura cross-coupling reaction on the irradiation wavelength. The numbers with percentages show the contribution of the light irradiation effect. Reaction conditions: Iodobenzene (0.125 mmol), phenylboronic acid (0.126 mmol), Pd (II) [PTATA G2-NH₂] @ TiO₂ (1.46 mol %) in H₂O: EtOH (0.5 ml) at room temperature after 30 min. This aim was gained using series of optical low-pass filters to block light below a specific cut-off wavelength. For example, the 450 nm optical filter blocks the wavelength below 450 nm and over 800 nm, in other words, the light irradiating the reactor has a wavelength range from 450 to 800 nm

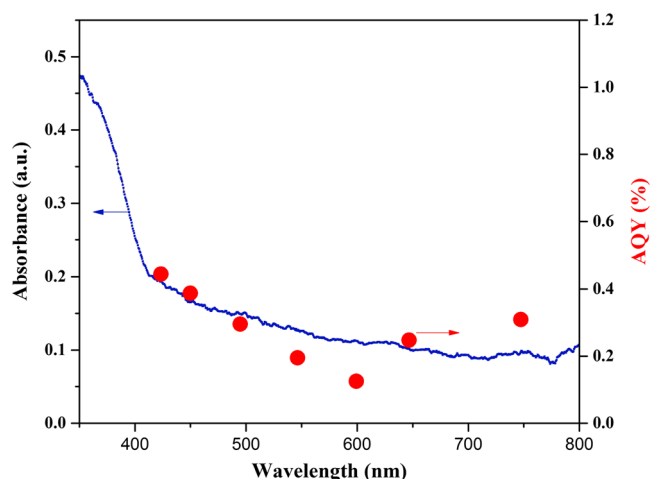


FIGURE 5 Photocatalytic action spectrum for synthesis of 4,4'-biphenyl using Pd (II) [PTATA G2-NH₂] @ TiO₂ photocatalyst in the Suzuki-Miyaura cross-coupling reaction

G2-NH₂] @TiO₂ under irradiation with different wavelengths (400 ± 5, 450 ± 5, 500 ± 5, 540 ± 5, 600 ± 5, 650 ± 5 and 750 ± 5) were determined. As shown in Figure 5, a good correlation is observed between AQY and the diffuse reflectance spectrum of the Pd (II) [PTATA G2-NH₂] @ TiO₂ in the reaction of the Suzuki-Miyaura cross-coupling reaction which confirms that the reactions are taking place photocatalytically.

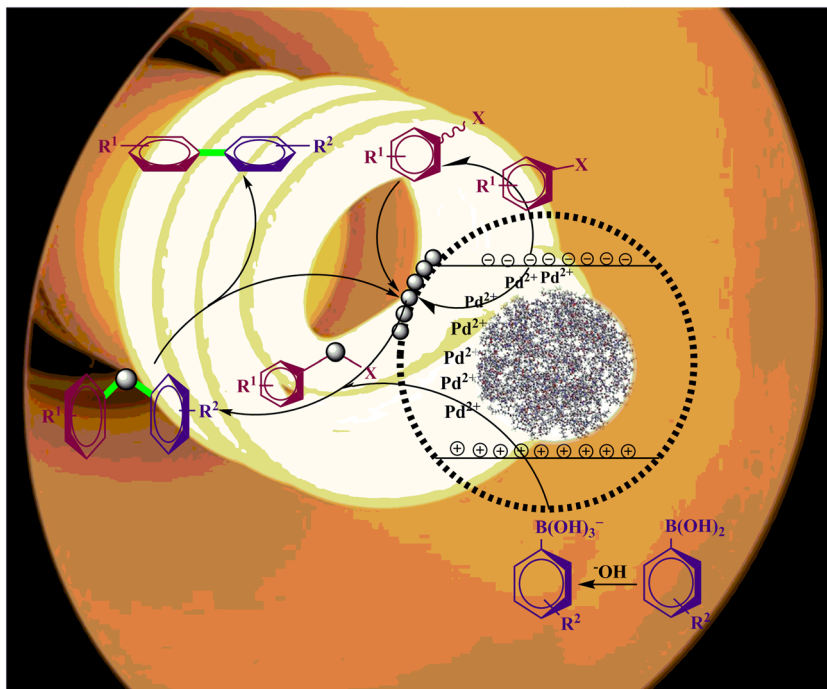
We then further tested the feasibility of Pd (II) [PTATA G2-NH₂] @ TiO₂ as nanodendritic photocatalysts for a series of Suzuki-Miyaura cross-

coupling reactions of phenylboronic acids with various aryl halides. Various p-substituted aryl halides, with groups such as -OMe, -Me, -NO₂ and substituted arylboronic acids (-Cl, -Et, -OMe, -CHO, -NO₂), were employed (Table 1) which gives the corresponding biphenyl compounds with good to high yields (52–96%) at room temperature within 30 minute to 3 h. As listed in Table 1, aryl iodides (for example entries 1–5,13–18), as expected, were converted more readily than their bromide and chloride counterparts (entries 6–10), which also showed good to excellent yields.

Also, this catalytic system shows great practical potential for the facile synthesis of terphenyls via one-pot double couplings of bihalide substrates with phenylboronic acid under the optimized reaction conditions (Table 1, entries, 11 and 12).

It was observed that Pd (II) [PTATA G2-NH₂] @ TiO₂ nanodendritic catalyst worked well for one pot triple coupling of cyanuric chloride and phenylboronic acid which leads to produce 1,3,5-triazine derivatives (Table 1, entry19). The 1,3,5-triazine derivatives as star-shaped compounds have been used in liquid crystals,^[68–70] component of organic light-emitting devices (OLEDs)^[71–73] coordination chemistry,^[74–76] and the syntheses of dendritic chromophores.^[77–79]

So, this method would offer the attraction of reducing the number of steps required to access highly aryl-substituted arenes. These results represent a significant advancement in the Suzuki-Miyaura cross-coupling reaction.



SCHEME 3 Proposed mechanism for the Suzuki-Miyaura cross-coupling catalyzed by Pd (II) [PTATA G2-NH₂] @TiO₂

A plausible reaction mechanism can be depicted as Scheme 3 on the basis of the above investigations and previous reports. Under visible light irradiation, nanodendritic catalyst can produce photo-generated electrons and holes. In principle, the energetic electrons and holes could activate the electron-deficient and electron-rich intermediates, respectively, to facilitate various organocatalytic reactions, including C–C coupling reactions.^[80] Palladium in Pd (II) [PTATA G2-NH₂] @TiO₂ nanodendritic catalyst under visible light irradiation is reduced to Pd(0). Oxidative addition of Pd(0) to the aryl halide (C–X) bonds takes place. On the other hand, arylboronic acid can acquire OH[−] in the basic reaction medium to form negative B(OH)₃[−] species, which is contribute to the trans-metalation process. Significantly, the h⁺ can assist in cleaving the C–B bond to produce biaryl-Pd complex (Scheme 3). In addition, to investigating of photogenerated electron–hole pairs, we carried out reaction between iodobenzene and phenylboronic acid in the presence of a hole scavenger such as ammonium oxalate (OA) and then a radical scavenger such as TEMPO which the desired product was obtained in 0% (No product) and 15% yield, respectively. Although, when the both of scavengers were used simultaneously, the yield of product was obtained in 10%. These studies propose that photogenerated hole and electron pair are crucial for carrying out the coupling reactions.

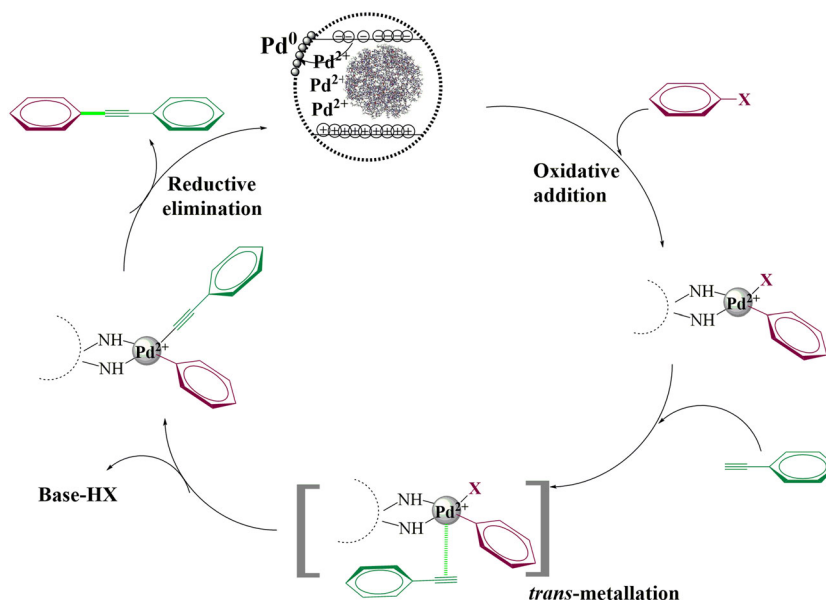
In continued, catalytic potential of title nanodendritic catalyst in the copper-free Sonogashira cross-coupling

reactions was investigated. There are many reports of catalytic activity palladium supported on composites as an efficient heterogeneous catalyst in the copper-free Sonogashira cross-coupling reactions.^[81–85] Preliminary investigations for the Sonogashira cross-coupling reactions were encouraging and the results are summarized in Table 2 (see the detail of optimizing conditions in supporting information Figure S8).

The catalytic activity of Pd (II) [PTATA G2-NH₂] @TiO₂ in the Sonogashira cross-coupling reaction is also dependent to the core type which acts as support, dendritic branches, and light wavelength and the results are depicted in Figure S9, S10, S11, S12.

On the basis of the evidence found in photocatalytic activity of title catalyst in the Suzuki–Miyaura and Sonogashira cross-coupling reactions, we propose that the improved photoactivity predominantly benefits from the synergistic effects of Pd (II) amine-terminated poly (triazine-triamine) dendritic on TiO₂ nanoparticles that cause efficient separation and photogenerated electron–hole pairs and photoredox capability of nanocatalyst which all of these advantages due to the tuning of band gap of catalyst in the visible light region.

In scheme 4, a possible catalytic reaction cycle for the copper-free Sonogashira reaction has been shown. At first, over the active Pd-sites present in TiO₂- supported heterogeneous catalyst, oxidative addition takes place, followed by transmetalation of alkyne and lastly reductive elimination of the final product.^[81]



SCHEME 4 Proposed mechanism for the Cu-free Sonogashira cross-coupling catalyzed by Pd (II) [PTATA G2-NH₂]@TiO₂

3.3 | Stability and reusability of catalyst

The reusability of Pd (II) [PTATA G2-NH₂]@TiO₂ catalyst was studied for Suzuki-Miyaura and Sonogashira cross-coupling reactions under optimized conditions. For this purpose, after completing of reactions, the title nanocatalyst (solid phase) was separated by centrifuging followed by decantation (3 × 5 ml ethanol). The catalyst was easily separated by centrifugation and reused in four consequent runs in the reactions (Figure S13). The FT-IR spectrum of the reused catalyst indicates that the structure of catalyst remained intact after recycling for both reactions (Figure S14).

Therefore, the title methodology is environmentally benign because of using visible light as an innocuous energy, reusing of an active catalyst with very low catalyst loading, easy isolation of organic products, and finally, no need for toxic reagents, or solvents.

4 | CONCLUSION

In conclusion, band gap of TiO₂ nanoparticles modified by Pd (II) amine-terminated poly (triazine-triamine) dendritic which induced outstanding photocatalytic activity in Suzuki-Miyaura and Sonogashira cross-coupling reactions under visible light at room temperature. This study shows that visible light irradiation can drive the cross-coupling reactions on the Pd (II) [PTATAD] @ TiO₂ under mild reaction conditions (27–30 °C) and no additional additives such as cocatalysts or phosphine ligands. While, the many reports of cross-coupling reactions have been catalyzed via homogeneous or heterogeneous processes that most of them need to be

conducted at elevated temperatures (≥ 100 °C), even under reflux conditions and additional additives. So, we propose that the improved photoactivity predominantly benefits from the synergistic effects of Pd (II) amine-terminated poly (triazine-triamine) dendritic on TiO₂ nanoparticles that cause efficient separation and photogenerated electron-hole pairs and photoredox capability of nanocatalyst which all of these advantages due to the tuning of band gap of catalyst in the visible light region.

ACKNOWLEDGMENTS

Support for this work by Research Council of University of Birjand is highly appreciated.

ORCID

Ameneh Eskandari  <https://orcid.org/0000-0001-9219-3994>

Maasoumeh Jafarpour  <https://orcid.org/0000-0002-9946-5013>

Abdolreza Rezaeifard  <https://orcid.org/0000-0002-8717-9036>

Mehri Salimi  <https://orcid.org/0000-0003-1755-7297>

REFERENCES

- [1] I. Hussain, J. Capricho, M. A. Yawer, *Adv. Synth. Catal.* **2016**, 358, 3320.
- [2] N. G. Schmidt, E. Eger, W. Kroutil, A. C. S. Catal, **2016**.
- [3] N. Corrigan, S. Shanmugam, J. Xu, C. Boyer, *Chem. Soc. Rev.* **2016**, 45, 6165.
- [4] C. C. C. Johansson Seechurn, M. O. Kitching, T. J. Colacot, V. Snieckus, *Angew. Chem. Int. Ed.* **2012**, 51, 5062.
- [5] M. Hartings, *Nat. Chem.* **2012**, 4, 764.

- [6] S. S. Stahl, *Science (80-)* **2005**, *309*, 1824.
- [7] J.-H. Kim, J.-W. Kim, M. Shokouhimehr, Y.-S. Lee, *J. Org. Chem.* **2005**, *70*, 6714.
- [8] J.-H. Kim, D.-H. Lee, B.-H. Jun, Y.-S. Lee, *Tetrahedron Lett.* **2007**, *48*, 7079.
- [9] M. Shokouhimehr, J.-H. Kim, Y.-S. Lee, *Synlett* **2006**, 2006, 618.
- [10] J. H. Park, F. Raza, S.-J. Jeon, H.-I. Kim, T. W. Kang, D. Yim, J.-H. Kim, *Tetrahedron Lett.* **2014**, *55*, 3426.
- [11] N. Miyaura, A. Suzuki, *Chem. Rev.* **1995**, *95*, 2457.
- [12] N. Miyaura, K. Yamada, A. Suzuki, *Tetrahedron Lett.* **1979**, *20*, 3437.
- [13] C. K. Prier, D. A. Rankic, D. W. C. MacMillan, *Chem. Rev.* **2013**, *113*, 5322.
- [14] K. L. Skubi, T. R. Blum, T. P. Yoon, *Chem. Rev.* **2016**, *116*, 10035.
- [15] M. D. Kärkäs, J. A. Porco Jr., C. R. J. Stephenson, *Chem. Rev.* **2016**, *116*, 9683.
- [16] F. Feizpour, M. Jafarpour, A. Rezaeifard, *Catal. Lett.* **2019**, *149*, 1595.
- [17] T. Yamada, H. Masuda, K. Park, T. Tachikawa, N. Ito, T. Ichikawa, M. Yoshimura, Y. Takagi, Y. Sawama, Y. Ohya, H. Sajiki, *Catalysts* **2019**, *9*, 461.
- [18] Q. Gu, Q. Jia, J. Long, Z. Gao, *Chem Cat Chem* **2019**, *11*, 669.
- [19] N. S. Lewis, D. G. Nocera, *Proc. Natl. Acad. Sci.* **2006**, *103*, 15729.
- [20] D. Gust, T. A. Moore, A. L. Moore, *Acc. Chem. Res.* **2001**, *34*, 40.
- [21] R. E. Blankenship, D. M. Tiede, J. Barber, G. W. Brudvig, G. Fleming, M. Ghirardi, M. R. Gunner, W. Junge, D. M. Kramer, A. Melis, others, *Science (80-)*. **2011**, *332*, 805.
- [22] N. Serpone, A. V. Emeline, **2012**.
- [23] H. Kisch, *Angew. Chem. Int. Ed.* **2013**, *52*, 812.
- [24] Z. Zhang, K. Edme, S. Lian, E. A. Weiss, *J. Am. Chem. Soc.* **2017**, *139*, 4246.
- [25] S.-J. Jeon, T.-W. Kang, J.-M. Ju, M.-J. Kim, J. H. Park, F. Raza, J. Han, H.-R. Lee, J.-H. Kim, *Adv. Funct. Mater.* **2016**, *26*, 8211.
- [26] F. Raza, J. H. Park, H.-R. Lee, H.-I. Kim, S.-J. Jeon, J.-H. Kim, *ACS Catal.* **2016**, *6*, 2754.
- [27] B. O'regan, M. Grätzel, *Nature* **1991**, *353*, 737.
- [28] P. Wang, S. M. Zakeeruddin, R. Humphry-Baker, J. E. Moser, M. Grätzel, *Adv. Mater.* **2003**, *15*, 2101.
- [29] S. Nakade, M. Matsuda, S. Kambe, Y. Saito, T. Kitamura, T. Sakata, Y. Wada, H. Mori, S. Yanagida, *J. Phys. Chem. B* **2002**, *106*, 10004.
- [30] M. R. Hoffmann, S. T. Martin, W. Choi, D. W. Bahnemann, *Chem. Rev.* **1995**, *95*, 69.
- [31] L. Gao, Q. Zhang, *Scr. Mater.* **2001**, *44*, 1195.
- [32] S. Y. Chae, M. K. Park, S. K. Lee, T. Y. Kim, S. K. Kim, W. I. Lee, *Chem. Mater.* **2003**, *15*, 3326.
- [33] K. Naoi, Y. Ohko, T. Tatsuma, *J. Am. Chem. Soc.* **2004**, *126*, 3664.
- [34] Y. Ohko, T. Tatsuma, T. Fujii, K. Naoi, C. Niwa, Y. Kubota, A. Fujishima, *Nat. Mater.* **2003**, *2*, 29.
- [35] Y. Lei, C. Zhang, H. Lei, J. Huo, *J. Colloid Interface Sci.* **2013**, *406*, 178.
- [36] A. W. Bosman, H. M. Janssen, E. W. Meijer, *Chem. Rev.* **1999**, *99*, 1665.
- [37] R. M. Crooks, M. Zhao, L. Sun, V. Chechik, L. K. Yeung, *Acc. Chem. Res.* **2001**, *34*, 181.
- [38] S. M. Grayson, J. M. J. Frechet, *Chem. Rev.* **2001**, *101*, 3819.
- [39] R. J. M. K. Gebbink, C. A. Kruithof, G. P. M. Van Klink, G. Van Koten, *Rev. Mol. Biotechnol.* **2002**, *90*, 183.
- [40] D. Astruc, E. Boisselier, C. Ornelas, *Chem. Rev.* **2010**, *110*, 1857.
- [41] S. Pan, S. Yan, T. Osako, Y. Uozumi, *ACS Sustain. Chem. Eng.* **2017**, *5*, 10722.
- [42] W. Zhang, D. T. Nowlan, L. M. Thomson, W. M. Lackowski, E. E. Simanek, *J. Am. Chem. Soc.* **2001**, *123*, 8914.
- [43] M. Nasr-Esfahani, I. Mohammadpoor-Baltork, A. R. Khosropour, M. Moghadam, V. Mirkhani, S. Tangestaninejad, H. Amiri Rudbari, *J. Org. Chem.* **2014**, *79*, 1437.
- [44] J. P. K. Reynhardt, Y. Yang, A. Sayari, H. Alper, *Chem. Mater.* **2004**, *16*, 4095.
- [45] A. V. Biradar, A. A. Biradar, T. Asefa, *Langmuir* **2011**, *27*, 14408.
- [46] A. L. Isfahani, I. Mohammadpoor-Baltork, V. Mirkhani, A. R. Khosropour, M. Moghadam, S. Tangestaninejad, R. Kia, *Adv. Synth. Catal.* **2013**, *355*, 957.
- [47] M. Jafarpour, F. Feizpour, A. Rezaeifard, *RSC Adv.* **2016**, *6*, 54649.
- [48] M. Jafarpour, A. Rezaeifard, F. Feizpour, *ChemistrySelect* **2017**, *2*, 2901.
- [49] M. Jafarpour, F. Feizpour, A. Rezaeifard, *Synlett* **2017**, *28*, 235.
- [50] M. Jafarpour, H. Kargar, A. Rezaeifard, *RSC Adv.* **2016**, *6*, 79085.
- [51] M. Jafarpour, H. Kargar, A. Rezaeifard, *RSC Adv.* **2016**, *6*, 25034.
- [52] M. Jafarpour, A. Rezaeifard, V. Yasinzadeh, H. Kargar, *RSC Adv.* **2015**, *5*, 38460.
- [53] P. Mpungose, Z. Vundla, G. Maguire, H. Friedrich, *Molecules* **2018**, *23*, 1676.
- [54] A. Khazaei, M. Khazaei, M. Nasrollahzadeh, *Tetrahedron* **2017**, *73*, 5624.
- [55] P. Puthiaraj, W.-S. Ahn, *Cat. Com.* **2015**, *65*, 91.
- [56] M. M. Heravi, E. Hashemi, Y. S. Beheshtiha, S. Ahmadi, T. Hosseinnejad, *J. Mol. Catal. A: Chem.* **2014**, *394*, 74.
- [57] M. Luo, C. Dai, Q. Han, G. Fan, G. Song, *Surf. Interface Anal.* **2016**, *48*, 1066.
- [58] D. A. Alonso, A. Baeza, R. Chinchilla, C. Gómez, G. Guillena, I. M. Pastor, D. J. Ramón, *Catalysts* **2018**, *8*, 202.
- [59] M. Esmaeilpour, S. Zahmatkesh, N. Fahimi, M. Nosratabadi, *Appl. Organomet. Chem.* **2018**, *32*, e4302.
- [60] M. Bagherzadeh, N. Mousavi, M. Zare, S. Jamali, A. Ellern, L. K. Woo, *Inorg. Chim. Acta* **2016**, *451*, 227.
- [61] M. Esmaeilpour, A. Sardarian, J. Javidi, *Cat. Sci. Technol.* **2016**, *6*, 4005.
- [62] R. Ciriminna, V. Pandarus, G. Gingras, F. Béland, P. Demma Carà, M. Pagliaro, *ACS Sustainable Chem. Eng.* **2012**, *1*, 57.
- [63] M. Jafarpour, M. Ghahramaninezhad, A. Rezaeifard, *New J. Chem.* **2014**, *38*, 2917.
- [64] P. A. Ajibade, O. G. Idemudia, *Bioinorg. Chem. Appl.* **2013**, *2013*, 549549.

- [65] M. Jafarpour, A. Rezaeifard, M. Ghahramaninezhad, T. Tabibi, *New J. Chem.* **2013**, 37, 2087.
- [66] Q. Xiao, S. Sarina, A. Bo, J. Jia, H. Liu, D. P. Arnold, Y. Huang, H. Wu, H. Zhu, *ACS Catal.* **2014**, 4, 1725.
- [67] Q. Xiao, Z. Liu, A. Bo, S. Zavahir, S. Sarina, S. Bottle, J. D. Riches, H. Zhu, *J. Am. Chem. Soc.* **2015**, 137, 1956.
- [68] J. M. Tour, *Chem. Rev.* **1996**, 96, 537.
- [69] C. Wang, A. S. Batsanov, M. R. Bryce, I. Sage, *Org. Lett.* **2004**, 6, 2181.
- [70] A. Błaszczak, M. Chadim, C. von Hänisch, M. Mayor, *European J. Org. Chem.* **2006**, 2006, 3809.
- [71] A. Hayek, F. Bolze, J.-F. Nicoud, P. L. Baldeck, Y. Mély, *Photochem. Photobiol. Sci.* **2006**, 5, 102.
- [72] F. Chérioux, A.-J. Attias, H. Maillotte, *Adv. Funct. Mater.* **2002**, 12, 203.
- [73] J. Wang, M. Lu, Y. Pan, Z. Peng, *J. Org. Chem.* **2002**, 67, 7781.
- [74] J. Pang, E. J.-P. Marcotte, C. Seward, R. S. Brown, S. Wang, *Angew. Chem. Int. Ed.* **2001**, 40, 4042.
- [75] A. de la Hoz, A. Díaz-Ortiz, J. Elguero, L. J. Martínez, A. Moreno, A. Sánchez-Migallón, *Tetrahedron* **2001**, 57, 4397.
- [76] P. K. Thallapally, R. K. R. Jetti, A. K. Katz, H. L. Carrell, K. Singh, K. Lahiri, S. Kotha, R. Boese, G. R. Desiraju, *Angew. Chem. Int. Ed.* **2004**, 43, 1149.
- [77] J. Palomero, J. A. Mata, F. González, E. Peris, *New J. Chem.* **2002**, 26, 291.
- [78] S. Achelle, Y. Ramondenc, F. Marsais, N. Plé, *European J. Org. Chem.* **2008**, 2008, 3129.
- [79] S. Kotha, D. Kashinath, K. Lahiri, R. B. Sunoj, *European J. Org. Chem.* **2004**, 2004, 4003.
- [80] X.-H. Li, M. Baar, S. Blechert, M. Antonietti, *Sci. Rep.* **2013**, 3, 1743.
- [81] K. Karami, S. Abedanzadeh, P. Hervés, *RSC Adv.* **2016**, 6, 93660.
- [82] M. Gholinejad, N. Dasvarz, C. Nájera, *Inorg. Chim. Acta* **2018**, 483, 262.
- [83] N. Li, R. K. Lim, S. Edwardraja, Q. Lin, *J. Am. Chem. Soc.* **2011**, 133, 15316.
- [84] A. Landarani Isfahani, I. Mohammadpoor-Baltork, V. Mirkhani, A. R. Khosropour, M. Moghadam, S. Tangestaninejad, *Eur. J. Org. Chem.* **2014**, 2014, 5603.
- [85] T. Saetan, C. Lertvachirapaiboon, S. Ekgasit, M. Sukwattanasinitt, S. Wacharasindhu, *Chem.–Asian J.* **2017**, 12, 2221.

SUPPORTING INFORMATION

Additional supporting information may be found online in the Supporting Information section at the end of the article.

How to cite this article: Eskandari A, Jafarpour M, Rezaeifard A, Salimi M. Supramolecular photocatalyst of Palladium (II) Encapsulated within Dendrimer on TiO₂ nanoparticles for Photo-induced Suzuki-Miyaura and Sonogashira Cross-Coupling reactions. *Appl Organometal Chem.* 2019; e5093. <https://doi.org/10.1002/aoc.5093>